

# RSC Advances



This is an *Accepted Manuscript*, which has been through the Royal Society of Chemistry peer review process and has been accepted for publication.

*Accepted Manuscripts* are published online shortly after acceptance, before technical editing, formatting and proof reading. Using this free service, authors can make their results available to the community, in citable form, before we publish the edited article. This *Accepted Manuscript* will be replaced by the edited, formatted and paginated article as soon as this is available.

You can find more information about *Accepted Manuscripts* in the [Information for Authors](#).

Please note that technical editing may introduce minor changes to the text and/or graphics, which may alter content. The journal's standard [Terms & Conditions](#) and the [Ethical guidelines](#) still apply. In no event shall the Royal Society of Chemistry be held responsible for any errors or omissions in this *Accepted Manuscript* or any consequences arising from the use of any information it contains.



Journal Name

COMMUNICATION

## Phosphonium based Ionic Liquids – Stabilizing or Destabilizing Agents for Collagen?

Received 00th January 20xx,  
Accepted 00th January 20xx

Aafiya Tarannum,<sup>a</sup> Charuvaka Muvva,<sup>a</sup> Ami Mehta,<sup>a</sup> J. Raghava Rao<sup>a</sup> and N. Nishad Fathima<sup>a</sup>

DOI: 10.1039/x0xx00000x

www.rsc.org/

**Abstract.** Collagen aids in preparation of biomaterials and its stability is a key factor for these applications. In this study, phosphonium based ionic liquids (PILs) was explored for its stability on collagen. The rheology of collagen, UV and fluorescence spectra slackens up with the increasing concentrations. CD and FT-IR spectra unveil the interaction of ions in ionic liquid with the collagen exhibiting the denaturation at higher levels. At the inter-fibrillar level, concentration dependent distortion in the banding pattern of RTT collagen fiber was observed due to the chaotropicity of ions. Molecular modeling studies also reveal the ions effect on the stability of collagen and structural deformation at higher concentration. Our results show that the ions play an active role at the level of interaction with protein towards stabilization or destabilization of collagen.

### 1. Introduction

Ionic liquids (ILs) are molten salts at room temperature. They are purely ionic, consisting solely of cations and anions<sup>1</sup>. A wide range of ionic liquids viz., ammonium, phosphonium, choline, imidazolium, pyrrolidinium, pyridinium, sulfonium<sup>2</sup> has been deliberately employed as electrolyte phases for biosensors<sup>3</sup>, medium for green synthesis<sup>4</sup> and protein preservation<sup>5</sup>. They have demonstrated stabilization of proteins by varying cations, anions and alkyl chains<sup>6</sup>.

Phosphonium cations paired with chloride and sulfonyl imide anions exhibit strong ion association, low viscosity and volatility<sup>7</sup>. They have shown better thermal stability and superior properties than ammonium based counter parts<sup>8</sup>. When phosphonium, ammonium and imidazolium are taken in consideration, the phosphonium RTILs prominently have the lower surface tension, varying of anions have the negligible effect<sup>9</sup>.

The changes in the native structure of BSA<sup>10</sup>, myoglobin<sup>11</sup> and insulin<sup>12</sup> with different ionic liquids have been explored. ILs

serves as a strong stabilizing medium for cytochrome C<sup>13</sup> and lysozyme<sup>14</sup> and nucleic acids<sup>15</sup> offering extended storage periods without the loss of activity. It was reported that choline ILs have been used considerably for protein-based pharmaceutical preparations and cellular therapies<sup>16</sup>. The anion of IL has an impact on the stability and activity of enzyme causing conformational changes as they strongly interact to alter functionality<sup>17</sup>.

Collagen has extensive applications for the preparation of biomaterials. The extended use of collagen brings out the need to understand the mechanism of stabilization, as they have utmost gaining significances for industrial and biological applications.

Interestingly, many ILs have been studied with collagen at different hierarchical ordering. It was reported that the choline DHP, a stabilizing agent for collagen can be used as a potential crosslinker<sup>18</sup>, whereas the ammonium and imidazolium<sup>19</sup> ILs have been denoted as destabilizing agents.

The purpose of the current investigation is to explore the stability of collagen with phosphonium based ionic liquids (PILs) and to study the effect of PILs on structure and conformational dynamics of collagen with varying anions such as tributyl methyl phosphonium methyl sulfate (PMS) and tributyl ethyl phosphonium diethyl phosphate (PEP) by different characterization techniques viz., viscosity analysis, circular dichroism (CD) studies, fourier transform infrared spectroscopy (FT-IR), UV and fluorescence, dimensional stability and impedance measurements. Further, to complement experimental studies, molecular dynamics simulation studies were performed.

### 2. Experimental Methods

#### 2.1 Materials

Rat tail tendon (RTT) excised from six month old albino rats (Wistar strain) were teased out. Tributyl methyl phosphonium methyl sulphate (PMS) and Tributyl ethyl phosphonium diethyl

<sup>a</sup>Chemical laboratory, CSIR-Central Leather Research Institute, Adyar, Chennai 600020, India.

E-mail: nishad@clri.res.in; nishad.naveed@gmail.com; Fax: +91 44 24911589; Tel: +91 4424411630

phosphate (PEP) (of 98% purity) were purchased from Ionic Liquid Technologies GmbH (IoLiTec) and used without further purification for this study. Millipore water was used for further studies. All other chemicals were of analytical grade.

## 2.2 Isolation of type I soluble collagen

Tails of six month old albino rats (Wistar strain) were excised as they are the rich source of high purity collagen. The teased collagen fibres were washed with 0.9% NaCl at 4°C. Collagen was extracted using acetic acid extraction method<sup>20</sup> and precipitated with 5% sodium chloride. The precipitate was collected by centrifugation was dialyzed extensively against 50mM phosphate buffer. The concentration of collagen in solution was determined from hydroxyproline content according to Woessner method<sup>21</sup>. The molar concentration of collagen was determined considering the average molecular weight of collagen as 300 kDa. The extracted collagen was used throughout the studies.

## 2.3 Preparation of collagen treated PILs

The working concentration of collagen estimated as 0.8 µM at pH 4. Phosphonium ionic liquid viz., Phosphonium methyl sulfate (PMS) and Phosphonium diethyl phosphate (PEP) was prepared at different ratio (1:0.05, 1:0.5, 1:5, 1:10) with collagen in acetate buffer under stirring for 3h at 4°C. The concentration of PILs was varied keeping the concentration of collagen constant.

## 2.4 Viscosity measurements

The viscosity of PILs treated collagen was performed using an Ostwald type Viscometer with 3 ml capacity. The flow times of collagen samples were measured after a thermal equilibrium time for 30 min. The collagen concentration was fixed and measurements were carried out with different concentration of ILs. It is based on the flow rate of collagen solution through capillary of an Ostwald viscometer. The flow time was measured with a digital stopwatch, each sample in a triplicate and the mean was taken. The viscosity ( $\eta_{rel}$ ) was calculated from the equation,

$$\eta_{rel} = \eta / \eta_0$$

Where,  $\eta$  is the time flow of buffer and  $\eta_0$  is the time flow of sample.

The collagen treated PILs were plotted on x-axis and  $\eta_{rel}$  on y-axis. ( $\eta_{rel} = 1/R$ ), ( $R = \text{Additive/Collagen}$ ).

## 2.5 UV-visible absorbance studies

PILs treated collagen was analyzed using UV-1800 Shimadzu (UV Visible spectrophotometer) with a quartz cuvette of 1.0-cm path length, assuring the proper determination of the baseline. The samples were incubated for overnight prior to

examination to study the interactions between native and PILs treated collagen.

## 2.6 Fluorescence measurements

Fluorescence spectra for PILs treated collagen were monitored on Cary Eclipse Fluorescence Spectrophotometer (Varian, Walnut Creek, USA) in a quartz cell. The excitation wavelength for collagen treated ILs was set at 275nm and emission was registered from 285 to 400nm with 5nm slit widths in both excitation and emission path at a scan rate of 100nm/min.

## 2.7 CD Spectroscopic studies

Far ultraviolet (190 nm to 260 nm) CD spectra for PILs treated collagen were obtained using Jasco 815 Circular dichroism spectropolarimeter in a quartz cell of volume 400 µl with a light path of 1 mm and scanned with 0.2 nm intervals at 25°C under nitrogen atmosphere with computer-averaged trace of three scans for each samples. The results were plotted with molar-residue-weight ellipticity ( $\text{deg.cm}^2.\text{dmol}^{-1}$ ) versus wavelength in nanometers (nm).

## 2.8 FT-IR Studies

Samples for FT-IR analysis were lyophilized under pressure of 6.4 Pa at -40°C. Prior to lyophilization all the PILs treated collagen samples were frozen by dipping in liquid N<sub>2</sub> and kept in the deep freezer for overnight. The wavelength dependent transmission intensity was characterized to observe the interactions between collagen and ionic liquids using Jasco FT/IR-4200 (Fourier Transform Infrared Spectrometer) with 60 scans in the range of 4000-400  $\text{cm}^{-1}$  at 25°C with a resolution of 4  $\text{cm}^{-1}$ .

## 2.9 Dimensional stability of RTT collagen fibres with PILs

Rat tail tendons (RTT) treated with ionic liquid for 24 h was observed under Aven Inc., Digital Mighty Scope, 1.3M (Product code: 48708-25, Made in Taiwan) of 10x resolution. The changes in the dimensional stability should be monitored.

## 2.10 Dielectric measurements

Impedance analysis for native and PILs treated collagen were carried out to determine the effect of ionic liquid on the resultant dipole of the protein molecule responding to an alternating electric field by means of CH Instrumental (USA) electrochemical analyzer CH-model 660 B with the three classical electrode system, where the glassy carbon electrode serves as a working electrode, a platinum electrode as a counter electrode and a saturated calomel electrode as a reference electrode. The operating conditions of dielectric were Init (E) = 90 mV, high frequency (f) = 10<sup>5</sup> Hz, low frequency (f) = 0.01 Hz, amplitude (V) = 0.005, Quiet time = 2S, cycles (0.01 – 0.1 Hz) = 1, cycles (0.001-0.01 Hz) = 1.

All the measurements were done in triplicates and average values are reported. Dielectric data can be represented in terms of admittance. The admittance  $Y''$  (unit:  $\Omega^{-1}$ ) can be written as

$$Y^* = Y' + jY''$$

Where  $Y'$  is the real component describing the energy stored and  $Y''$  is the imaginary component depicting the energy dissipated by the system. All the measurements were repeated for three times for reproducibility.

### 2.11 Molecular modelling studies

To understand the structural behaviour of collagen at different concentrations of PMS and PEP, classical molecular dynamics simulation were performed. The structure of collagen like peptides was constructed using the gencollagen package<sup>22</sup>. The molecular dynamics simulation was carried out using GROMACS (version 4.6.2)<sup>23, 24</sup> package employing the AMBER03 force field<sup>25</sup> for collagen was used. The geometries of the AMS compound were fully optimized using B3LYP/6-31G(d,p) level and their electrostatic potentials were obtained using same level of theory, using the GAUSSIAN 09 package<sup>26</sup>. The force field was generated using the Antechamber module of amber package<sup>27, 28</sup> and RESP charges were generated for PMS and PEP compound. Each model was solvated with TIP3P water molecules in a cubic box<sup>29</sup>. All models were subjected to energy minimization using the steepest decent method to relax the entire system. The production run was carried out for all the systems for 100 nanoseconds (ns) using 2 femtoseconds time step for integration of equation of motion in NPT ensemble at 300 K and at 1 atmospheric pressure, which was controlled using a V-rescale thermostat and Parrinello–Rahman Barostat respectively<sup>30-32</sup>. The particle mesh Ewald (PME) was used to calculate the electrostatic interaction with the cutoff of 10 Å. The trajectories obtained from MD simulations were visualized with the help of the VMD package<sup>33</sup>. Further analysis of trajectories was performed with the tools available in the GROMACS package.

The peptide sequence for collagen used for modelling in this study is,

GPOGKOGPOGPOGPOGROGPOGAOGHOGSO  
GPOGKOGPOGPOGPOGROGPOGAOGHOGSO  
GPOGKOGPOGPOGPOGROGPOGAOGHOGSO

This proposed sequence was developed by Object Technology Framework (OTF) using the GENCOLLAGEN package<sup>34</sup>. This sequence was chosen for modelling, as these amino acid residues play a significant role in interacting with the additives and it alters the microenvironment of collagen.

## 3. RESULTS AND DISCUSSION

### 3.1 Effect of PILs on the rheology of collagen – Viscosity measurements

In order to understand the influence of PILs on the rheological behaviour of collagen, viscosity measurements were carried out<sup>35</sup>. The rheological property reflects the strength of inter- and intra-molecular forces; the stronger the force the higher will be the viscosity. Relative viscosity for collagen was studied with the varying concentration of PILs. Figure S1 exhibits the rheological behaviour for collagen-PILs, which demonstrated the change in the relative viscosity ( $\eta_{\text{relative}}$ ) with the addition of PIL. The  $\eta_{\text{relative}}$  was found to increase with increasing PIL concentration. Hence, the rheology for PEP and PMS treated collagen shows the higher tendency to aggregate. The increasing viscosity with increase in concentration of PILs generally attributes to aggregation.

### 3.2 Effect of PILs on the microenvironment of collagen – UV absorption studies

The sensitivity of tyrosine to its chemical environment makes this amino acid a highly important spectroscopic probe for conformations and dynamics. In this context, the absorption spectra of biomacromolecule have been made the subject of considerable study. In the UV region, the peak at 205 nm indicates peptide absorption peak in protein, whereas a second weak absorption peak at about 278 nm is due to aromatic amino acids<sup>36</sup>.

As seen from Figure S2a, at 278 nm for phosphonium methyl sulfate (PMS), an increase in absorbance intensity was observed for C-PMS-1 and C-PMS-2 than native collagen which might be due to the least interaction of collagen with PMS, whereas the C-PMS-3 and C-PMS-4 ascribes the decrease in absorbance intensity indicating changes in the microenvironment of collagen. This might be due to the ions, which interacts strongly with collagen at higher concentration of PMS causing the structural deformation.

In Adjunct, Figure S2b demonstrated a decrease in the absorbance with the increase in concentration of C-PEP-2, C-PEP-3 and C-PEP-4, implying the complete loss of tyrosine environment which may be due to direct interaction of PEP, thereby resulting in denaturation of collagen.

### 3.3 Effect of PILs on the fluorescence spectra of collagen

The tyrosine environment of native collagen and collagen in PILs was analyzed by fluorescence spectroscopy. Figure S3a phosphonium methyl sulfate (PMS) shows the emission of tyrosine residues at 305 nm with increased fluorescence up to C-PMS-2. The lack of characteristic peak for C-PMS-3 and C-PMS-4 records the absence of tyrosine emission. This could be due to denaturation of collagen at higher concentration. In Figure S3b phosphonium diethyl phosphate (PEP), the strong emission of tyrosine residue was seen at 305 nm, revealing an increase in intensity till C-PEP-3. The absence of characteristic peak for C-PEP-4 at 305 nm was observed, which might be due

to the movement of tyrosine residues, resulting in defragmentation of molecules tapering aggregation of collagen.

### 3.4 Effect of PILs on the secondary structure of collagen – CD spectral studies

In order to understand whether PILs influence the secondary structure of collagen, CD spectral studies on collagen/PILs were carried out<sup>37, 38</sup>. Figure 1a and 1b describes the CD spectra of collagen of two PILs at different concentrations. Phosphonium methyl sulphate (PMS) and phosphonium diethyl phosphate (PEP) alone do not show any spectra in the range 190-260 nm, indicating that the observed CD spectrum is due to collagen. In the far UV region, pure collagen exhibits its minimum at 197 nm and maximum at 222 nm, authenticating a typical polyproline type II (PPII) conformation. C-PMS-1 and C-PMS-2 recorded the increased ellipticity so as C-PEP-1 and C-PEP-2 due to least interaction and lesser hydrogen bonding of collagen with the ions present in PILs. The acerbic change with increasing concentration of PILs, C-PMS/PEP-3 and C-PMS/PEP-4 has shown decrease in molar ellipticity values compared to native, which might be due to the increased hydrogen bonding ability of ions indicating a strong interaction resulting in denaturation of collagen structure. A marginal increase in the molar ellipticity value suggesting negligible effect on the secondary structure of collagen was witnessed for imidazolium ILs<sup>19</sup>, albeit a remarkable increase in molar ellipticity of collagen treated with choline ILs<sup>18</sup> was observed, indicating stability of collagen. Altered changes in the CD spectra of collagen treated PILs exhibit that the interaction with collagen affects the structure of collagen at higher levels.

### 3.5 Effect of PILs on the alteration of functional groups of collagen – FT- IR spectral studies

Infrared (IR) spectroscopy detects the vibration characteristics of functional groups in a sample. A functional group tends to absorb IR radiation in a specific wave number ( $\text{cm}^{-1}$ ) range<sup>39, 40</sup>. The presence or absence of peaks within the region discerns the structural information regarding the molecule. Collagen shows characteristic FT-IR spectrum, with absorption bands of N-H and O-H stretching at  $3300 \text{ cm}^{-1}$  for amide A, C-H stretching at  $2948 \text{ cm}^{-1}$  for amide B, C=O stretching at  $1640 \text{ cm}^{-1}$  for Amide I, N-H bending and C-H stretching at  $1560 \text{ cm}^{-1}$  for amide II, carboxyl OH at  $1240 \text{ cm}^{-1}$  for amide III. It is known that amide I and II bands are attributed to polyproline type II structure of collagen. Figure 2a and 2b discloses the slight shift in amide A band, O-H stretching to higher frequencies ( $3280 \text{ cm}^{-1}$ ) for C-PMS/PEP (1-4), this may have arisen from the least interaction of hydrogen bonds within collagen molecules resulting from the interaction between collagen and PMS/PEP compared to that of native collagen ( $3279 \text{ cm}^{-1}$ ). Also, the amide I is centred around  $1635 \text{ cm}^{-1}$ , indicating C=O stretching for collagen treated PMS, whereas the shift in the peaks was observed around  $1631 \text{ cm}^{-1}$  for C-PEP-3 and C-PEP-4. This

might be due to the burying of hydrophilic groups in the interior core of collagen at higher concentrations. N-H bending and C-H stretching for amide II was seen at  $1561 \text{ cm}^{-1}$  for native, but there was a variation in the corresponding concentration of C-PMS and C-PEP, which was signalled around  $1550$  and  $1545 \text{ cm}^{-1}$  respectively. However there was abrupt change witnessed in amide III band for C-PEP-4 with the shift from  $1241 \text{ cm}^{-1}$  to  $1224 \text{ cm}^{-1}$  and for C-PMS-4 there was drastic shift witnessed from  $1241 \text{ cm}^{-1}$  to  $1229 \text{ cm}^{-1}$  indicating a plausible interaction of collagen with ionic liquids, altering the microenvironment of collagen, which in turn causes the disruption in structure. In the case of imidazolium ILs<sup>19</sup>, there was slight shift in amide I, II and III bands indicating tenuous change in secondary structure of collagen, whereas the shifts in choline ILs<sup>18</sup> indicated increased physical crosslinks.

Amide bands of the FT-IR spectra are sensitive to the secondary structure of collagen. Changes in the position of amide of collagen clarifies that the secondary structure of collagen is altered, which indicates aggregation or compactness. From the experimental observations it was concluded that the ions have high hydrogen bond forming capability and it strongly interact with collagen, which causes the conformational changes in structure which can be further confirmed through molecular dynamics studies.

### 3.6 Effect of PILs on the dimensional stability of RTT collagen fibres

Rat tail tendons (RTT) known to be the rich source of type I collagen fibres were excised from albino rats. It shows the characteristic macroscopic banding pattern in aqueous medium that reveals the helicity of fibrils<sup>41</sup>. Figure 3 explicates the treatment of RTT with phosphonium diethyl phosphate (PEP) and phosphonium methyl sulfate (PMS), with varying concentrations (0.05%, 0.5%, 5% and 10%) it unveils the huge impact on dimensional stability of RTT collagen fibres. It was observed that there was a remarkable distortion of wave pattern within the first hour of incubation and no change were analyzed in the later hours, whereas for imidazolium ILs<sup>19</sup>, it have shown slight swelling effect, it may be due to increased surface tension at the water-IL interface, albeit the choline<sup>18</sup> ILs shows no swelling effect indicating stabilization. The drastic distortion in wave pattern for PILs could be due to the chaotropicity of ions that alter the structure of water molecule, leading to agglomeration, defragmentation and destabilization of RTT collagen fibres.

### 3.7 Dielectric measurements

AC impedance measurement aids in determining nature of hydrated components in protein through its dielectric response under electric field. Collagen composites with different concentrations of PILs were subjected for impedance measurement to determine the dielectric properties and hydration behaviour of biomacromolecules<sup>42, 43</sup>. The dielectric technique is particularly sensitive to analyze the dynamic characteristics of water. This phenomenon will have an effect

on conformation of collagen in the presence of phosphonium class of ionic liquids. Nyquist admittance plot demonstrates the capability to trap electric charge through steepness of circles whereas Debye relaxation model explains the polarization behaviour as a response to electric charge entrapped. Figure 4a shows the Nyquist plot for C-PMS discerning the admittance plotted using real  $Y'$  vs. imaginary  $Y''$ . Concentration dependent increased permittivity was observed for the C-PMS, whereas the collagen shows the lowest permittivity. This is owing to the fact that collagen is a protein with various functional groups, which leads to its charged behaviour. For collagen/PMS (1-4), there was an increase in permittivity with the increasing concentration of PMS treated collagen. Bode plot, figure 4b of collagen, C-PMS-1 and C-PMS-2 shows a phase angle at high frequency of about  $10^3$  Hz. For C-PMS-3 and C-PMS-4, phase angle is increased to higher frequencies, from  $10^3 - 10^5$  Hz. This change in frequency owing to the addition of PMS was likely due to interaction of charged functional groups of collagen with PMS. The result indicates that the dielectric behaviour of collagen-PMS is due to the displacement of charges.

Figure 4c depicts the Nyquist plot for PEP treated collagen, revealing the admittance for biomacromolecule. Native collagen show the lowest permittivity, whereas the PEP treated collagen records the concentration dependent permittivity. This may be due to the reorganization of bound water molecules in the proteins and there is strong influence of additives in it. Bode plot, figure 4d shows a phase angle at high frequency of about  $10^3$  Hz for native collagen, C-PEP-1 and C-PEP-2, albeit for C-PEP-3 and C-PEP-4 phase angle is shifted to higher frequencies from  $10^3 - 10^5$  Hz, suggesting that there is a high probability of charge transfer between the amino acids of the protein, ions present in ionic liquid and water molecules. It clearly explains the bound charges of the protein when comes in contact with dielectric current results in reorientation and reorganization in the network of proteins.

### 3.8 Molecular Dynamics Simulation studies

The molecular dynamics simulation studies were carried out for collagen upon its interaction with phosphonium methyl sulphate (PMS) and phosphonium diethyl phosphate (PEP). Molecular docking studies for choline ILs indicated that the interaction between choline ILs<sup>18</sup> and collagen was electrostatic in nature, which was likely to have promoted stability. In this study, root mean square deviation (RMSD), root mean square fluctuation (RMSF), hydrogen bonding analysis, radial distribution analysis and spatial distribution analysis have been demonstrated to complement experimental techniques.

#### 3.8.1 Effect of PILs on Root Mean Square Deviation (RMSD) and Root Mean Square Fluctuation (RMSF)

In order to understand the effects of various concentrations of PMS and PEP on the collagen structure, the Root Mean Square Deviation (RMSD) was calculated<sup>44</sup>. The structural deviations in collagen were calculated with the help of RMSD with reference to its initial structure. The changes in RMSD values with time for various models are given in figure 5a and 5b. It reveals the significant changes in the RMSD within the models. It can be noted that there are slight structural deviations compared to its initial structure of collagen in the presence of PMS and PEP. There was negligible difference in the RMSD values for both PMS and PEP. It was also observed that RMSD of all the systems increases up to 7 Å due to winding and unwinding of triple helical peptide throughout the MD simulation. However, there was a witnessing increase in the RMSD values with the increasing concentration, which might be due to the structural deformity and it is confirmed using other MD studies.

To understand the effect of PMS and PEP of varied concentrations on the structural stability of collagen, RMSF of C $\alpha$  residues from its time averaged position was computed. Figure 6a and 6b illustrates the slight changes in RMSF of collagen, whereas a huge residual fluctuation was observed for higher concentrations of PMS and PEP, with an increase in increasing concentrations of PMS and PEP. These results suggest the noticeable change in flexibility of collagen with the increasing concentration of phosphonium ILs.

#### 3.8.2 Effect of PILs on hydrogen bonding

The H-bonding is one of the major interactions which stabilize the triple helical structure of collagen. The number of hydrogen bonds formed between collagen and PMS, PEP (cation and anion) models during MD simulation was calculated<sup>45, 46</sup>. Figure 7a and 7b elucidates that there was no hydrogen bonding between collagen and PMS (cation) for C-PMS-1 to C-PMS-4. In the case of C-PEP-1 to C-PEP-4, there was negligible interaction between collagen and PEP (cation) and upon increasing the concentration there exist no noticeable change in the structure of collagen.

For C-PMS-1 and C-PMS-2 (anion) only few hydrogen bonds were observed and there was an increase in the number of hydrogen bonds with increase in concentration of PMS which was seen from figure 7c and 7d. On average 20 hydrogen bonds were observed for C-PMS-3 and C-PMS-4. On the other hand for C-PEP-1 to C-PEP-4, there was an increase in the formation of hydrogen bonds with the increasing concentration of PEP. From hydrogen bonding analysis, it was evident that at higher concentrations of C-PMS and C-PEP (anion) the number of hydrogen bonds increased drastically leading to strong interaction between collagen and PMS, PEP (anion), which might be the reason for structural deformation of collagen. It is elucidated that anions play a major role in structural deformity of collagen, whereas cations show negligible effect. The anion of IL has an impact on the protein stability and activity. Generally, it was observed that anion having high hydrogen bond forming capability, which strongly interacts with protein causing the conformational change in the structure, the stronger the

bonding, the higher will be interaction with the marked changes in the structure of proteins.

These outcomes clearly abide with FT-IR, CD and viscosity analysis, which states that the interaction of collagen with increased concentration of PEP and PMS leads to collagen denaturation.

### 3.8.3 Effect of PILs on radial distribution function (RDF)

To assess the distribution of PMS and PEP molecules in varied concentration, radial distribution analysis (RDF) was calculated for PMS and PEP (cation and anion) around the collagen. From the figure 8a and 8b, it was observed that for PMS (cation) at lower concentration the height of the peak is around 1.3 nm, which increases slightly with respect to increase in concentrations of PMS (cation). In the case of PEP (cation), the values are slightly higher than PMS (cation) and it was centred on 1.5 nm.

Figure 8c exhibits that PMS (anion) value of  $g(r)$  is high and it is within 0.7 nm for C-PMS-1 and C-PMS-2. There was a decrease in  $g(r)$  values with the increase in concentration of PMS (anion). As seen from figure 8d, PEP (anion) witnessed the higher value for lower concentration of PEP, which was around 0.7 nm. There was a drastic decrease in  $g(r)$  values for C-PEP-3 and C-PEP-4. The results clearly show that the interaction of anions with collagen is more when compared to the cation, as there was acerbic change in  $g(r)$  values for both PMS and PEP (anion). It can be concluded that cations are not much implied, whereas the anions of PEP and PMS are hugely involved in interaction and causes structural disruption.

### 3.8.4 Effect of PILs on spatial distribution function (SDF)

In order to explicate the interaction and distribution of cations and anions around collagen, spatial distribution analysis (SDF) has been carried out. It usually accounts for the dynamics of water and IL system around the protein<sup>46</sup>. Figure 9 describes the spatial distribution of ions around collagen for averaged 100 ns simulation. On analyzing the SDFs, we observed that there was a strong interaction of anions of PMS and PEP with the positively charged residues of collagen, synonymously with an efficient anion scattered around the protein surface. This is shown by different isovalues used to represent the distribution of cations and anions around collagen. Most notably, high concentrations of PMS and PEP (anion) (figure 9b and 9d) showed stronger interaction indicating structural deformity. The prevalence of PMS and PEP (cation) (figure 9a and 9c) also show slight effect, indicating the interaction of cation with collagen may also cause structural changes. Overall, these results are in accordance with the fact that the anions play a major role in destabilizing collagen for higher concentration of PMS and PEP and it was in accord with other experimental techniques.

## 4. Conclusion

The current investigation implies evidence of the destabilizing effect of PILs on collagen, witnessing the rheology of collagen to the variance in the fluorescence and absorption spectra observed for increasing concentration, with the CD spectra depicting the decrease in ellipticity values to the lower intensities of the bands in the FT-IR spectral studies and optical micrograph, which predicates slacking up of collagen. The physico-chemical properties are varied in the complete denaturation process due to the stronger interaction of hydrogen bonds of collagen with ions resulting to denatured state. The molecular modelling studies also reveal that the anions are responsible for structural deformation of collagen and it was in accord with other experimental techniques. Hence, it clearly entails that the PILs interaction with the collagen destabilizes the structure. In addition, further studies are underway to determine better interactions between ionic liquids and collagen for the stabilization process which will broaden the IL applications.

## Acknowledgement

We, the authors thank CSIR – Research Initiatives for Waterless Tanning (RIWT) project for the fellowship (CSC0202). CSIR-CLRI communication code: 1178. We also thank Dr. V. Subramanian for his insights and support towards our research. We are grateful to C-MMACS for providing super-computing facility to carry out this work.

## Notes and references

- 1 J. K. Fraser, D. R. MacFarlane, *Aust. J. Chem.*, 2009, **62**, 309.
- 2 K. Petkovic, K. R. Seddon, L. P. N. Rebelo, C. S. Pereira, *Chem. Soc. Rev.*, 2011, **40**, 1383.
- 3 D. Wei, A. Ivaska, *Anal. Chim. Acta.*, 2008, **607**, 126.
- 4 M. Moniruzzamana, K. Nakashimab, N. Kamiyaa, M. Goto, *Biochem. Eng. J.*, 2010, **48**, 295.
- 5 R. A. Judge, S. Takahashi, K. L. Longnecker, E. H. Fry, C. A. Zapatero, M. L. Chiu, *Cryst. Growth. Des.*, 2009, **9**, 3463.
- 6 M. Naushad, Z. A. ALOthman, A. B. Khan, M. Ali, *Int. J. Biol. Macromolec.*, 2012, **51**, 555.
- 7 K. J. Fraser, E. I. Izgorodina, M. Forsyth, J. L. Scott, D. R. MacFarlane, *Chem. Commun.*, 2007, 3817.
- 8 T. J. Wooster, K. M. Johanson, K. J. Fraser, D. R. MacFarlane, J. L. Scott, *Green. Chem.*, 2006, **8**, 691.
- 9 P. Kilaru, G. A. Baker, P. Scovazzo, *J. Chem. Eng. Data.*, 2007, **52**, 2306.
- 10 L. Y. Zhu, G. Q. Li, F. Y. Zheng, *J. Biophys. Chem.*, 2011, **2**, 146.
- 11 K. Sankaranarayanan, G. Satharaj, B. U. Nair, A. Dhathathreyan, *J. Phys. Chem. B.*, 2012, **116**, 4175.
- 12 A. Kumar, P. Venkatesu, *RSC Adv.*, 2014, **4**, 4487.
- 13 K. Fujita, D. R. MacFarlane, M. Forsyth, M. Y. Fujita, K. Murata, N. Nakamura, H. Ohno, *Biomacromolecules*, 2007, **8**, 2080.
- 14 J. V. Rodrigues, V. Prosinecki, I. Marrucho, L. P. N. Rebelo, C. M. Gomes, *Phys. Chem. Chem. Phys.*, 2011, **13**, 13614.
- 15 H. T. Karimata, N. Sugimoto, *Nuc. Acids. Res.*, 2014, **42**, 8831.
- 16 J. Ranke, S. Stolte, R. Stormann, J. Arning, B. Jastorff, *Chem. Rev.*, 2007, **107**, 2183.

- 17 H. Zhao, *J. Chem. Tech. and Biotech.*, 2010, **85**, 891.
- 18 A. Mehta, J. R. Rao, N. N. Fathima, *J. Phys. Chem. B.*, 2015, **119**, 12816.
- 19 A. Mehta, J. R. Rao, N. N. Fathima, *Colloids. Surf. B.*, 2014, **117**, 376.
- 20 G. Chandrakasan, D. A. Torchia, K. A. Priez, *J. Biol. Chem.*, 1976, **251**, 6062.
- 21 J. F. Woessner, *Arch. Biochem. Biophys.* 1961, **93**, 440.
- 22 [http://www.cgl.ucsf.edu/cgi-bin/gencollagen.py]. The GenCollagen Database
- 23 H. J. C. Berendsen, D. Vander Spoel, R. Van Drunen, *Comput. Phys. Commun.*, 1995, **91**, 43.
- 24 B. Hess, C. Kutzner, D. Vander Spoel, E. Lindahl, *J. Chem. Theory Comput.*, 2008, **4**, 435.
- 25 Y. Duan, C. Wu, S. Chowdhury, M. C. Lee, G. M. Xiong, W. Zhang, R. Yang, P. Cieplak, R. Luo, T. Lee, J. Caldwell, J. M. Wang, P. Kollman, *J. Comput. Chem.*, 2003, **24**, 1999.
- 26 M. J. Frisch, G. W. Trucks, H. B. Schlegel, G. E. Scuseria, M. A. Robb, J. R. Cheeseman, G. Scalmani, V. Barone, B. Mennucci, G. A. Petersson, H. Nakatsuji, M. Caricato, X. Li, H. P. Hratchian, A. F. Izmaylov, J. Bloino, G. Zheng, J. Sonnenberg, M. Hada, M. Ehara, K. Toyota, R. Fukuda, J. Hasegawa, M. Ishida, T. Nakajima, Y. Honda, O. Kitao, H. Nakai, T. Vreven, J. A. Montgomery, J. E. Peralta, F. Ogliaro, M. Bearpark, J. J. Heyd, E. Brothers, K. N. Kudin, V. N. Staroverov, R. Kobayashi, J. Normand, K. Raghavachari, A. Rendell, J. C. Burant, S. S. Iyengar, J. Tomasi, M. Cossi, N. Rega, J. M. Millam, M. Klene, J. E. Knox, J. B. Cross, V. Bakken, C. Adamo, J. Jaramillo, R. Gomperts, R. E. Stratmann, O. Yazyev, A. J. Austin, R. Cammi, C. Pomelli, J. W. Ochterski, R. L. Martin, K. Morokuma, V. G. Zakrzewski, G. A. Voth, P. Salvador, J. J. Dannenberg, S. Dapprich, A. D. Daniels, J. Farkas, B. Foresman, J. V. Ortiz, J. Cioslowski, D. J. Fox, Gaussian 09, Revision A. 02; Gaussian, Inc.: Wallingford, CT, 2009.
- 27 J. Wang, W. Wang, P. Kollman, D. A. Case, *J. Mol. Graphics Modell.*, 2006, **25**, 247.
- 28 J. Wang, R. M. Wolf, J. W. Caldwell, P. A. Kollman, D. A. Case, *J. Comput. Chem.*, 2004, **25**, 1157.
- 29 W. L. Jorgensen, J. Chandrasekhar, J. D. Madura, R. W. Impey, M. L. Klein, *J. Chem. Phys.*, 1983, **79**, 926.
- 30 M. Parrinello, A. Rahman, *J. Appl. Phys.*, 1981, **52**, 7182.
- 31 S. Nosé, M. L. Klein, *Mol. Phys.*, 1983, **50**, 1055.
- 32 G. Bussi, D. Donadio, M. Parrinello, *J. Chem. Phys.*, 2007, **126**, 014101.
- 33 W. Humphrey, A. Dalke, K. Schulten, *J. Mol. Graphics.*, 1996, **14**, 33.
- 34 C. C. Huang, G. S. Couch, E. F. Pettersen, T. E. Ferrin, A. E. Howard, T. E. Klein, *Pac. Symp. Biocomput.*, 1998, 349.
- 35 N. N. Fathima, A. Dhathathreyan, *Int. J. Biol. Macromolec.*, 2009, **45**, 274.
- 36 N. O. Metrevel, K. K. Jariashvili, L. O. Namicheishvili, D. V. Svintradze, E. N. Chicvaidze, A. Sionkowska, *Ecotox. Env. Saf.*, 2010, **73**, 448.
- 37 N. J. Greenfield, *Trends. Anal. Chem.*, 1999, **18**, 236.
- 38 S. M. Kelly, T. J. Jess, N. C. Price, *Biochim. Biophys. Acta.*, 2005, **1751**, 119-139.
- 39 B. C. Vidal, M. Luiza, S. Mello, *Micron.*, 2011, **42**, 283.
- 40 A. Barth, *Biochim. Biophys. Acta.*, 2007, **1767**, 1073.
- 41 A. Mehta, J. R. Rao, N. N. Fathima, *Int. J. Biol. Macromolec.*, 2014, **4346**, 1.
- 42 I. Kanungo, N. N. Fathima, J. R. Rao, B. U. Nair, *Mat. Chem. and Physico.*, 2013, **140**, 357.
- 43 I. S. Raja, N. N. Fathima, *SpringerPlus.*, 2014, **3**, 393.
- 44 E. R. Azhagiya Singam, K. Balamurugan, R. Gopalakrishnan, S. R. Subramanian, V. Subramanian, T. Ramasami, *Biopolymers.*, 2012, **97**, 847.
- 45 E. Schreiner, C. Nicolini, B. Ludolph, R. Ravindra, N. Otte, A. Kohlmeyer, R. Rousseau, R. Winter, D. Marx, *Phys. Rev. Lett.*, 2004, **92**, 148101.
- 46 A. M. Figueiredo, J. Sardinha, G. R. Moore, E. J. Cabrita, *Phys. Chem. Chem. Phys.*, 2013, **15**, 19632.

## FIGURES

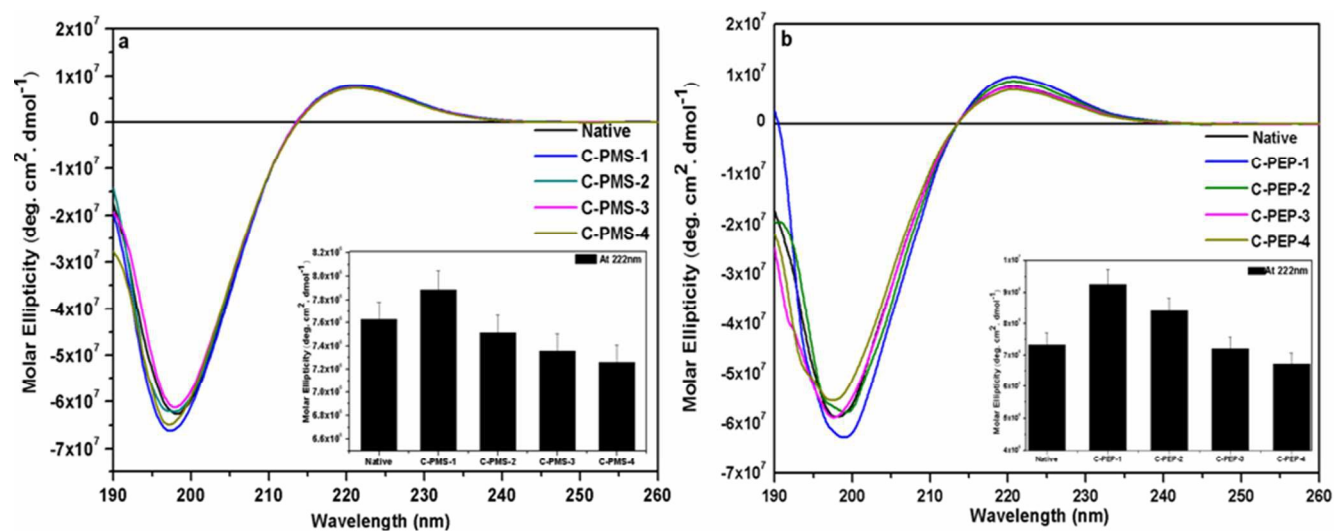


Figure 1. Conformational changes in the far - UV CD spectra of collagen (Molar Ellipticity values at 222nm for collagen treated with PILs at different molar ratios in the inset) (a) C-PMS-1 to C-PMS-4 (Collagen: Phosphonium methyl sulfate 1:0.05% to 1:10%) (b) C-PEP-1 to C-PEP-4 (Collagen: Phosphonium diethyl phosphate 1:0.05% to 1:10%)

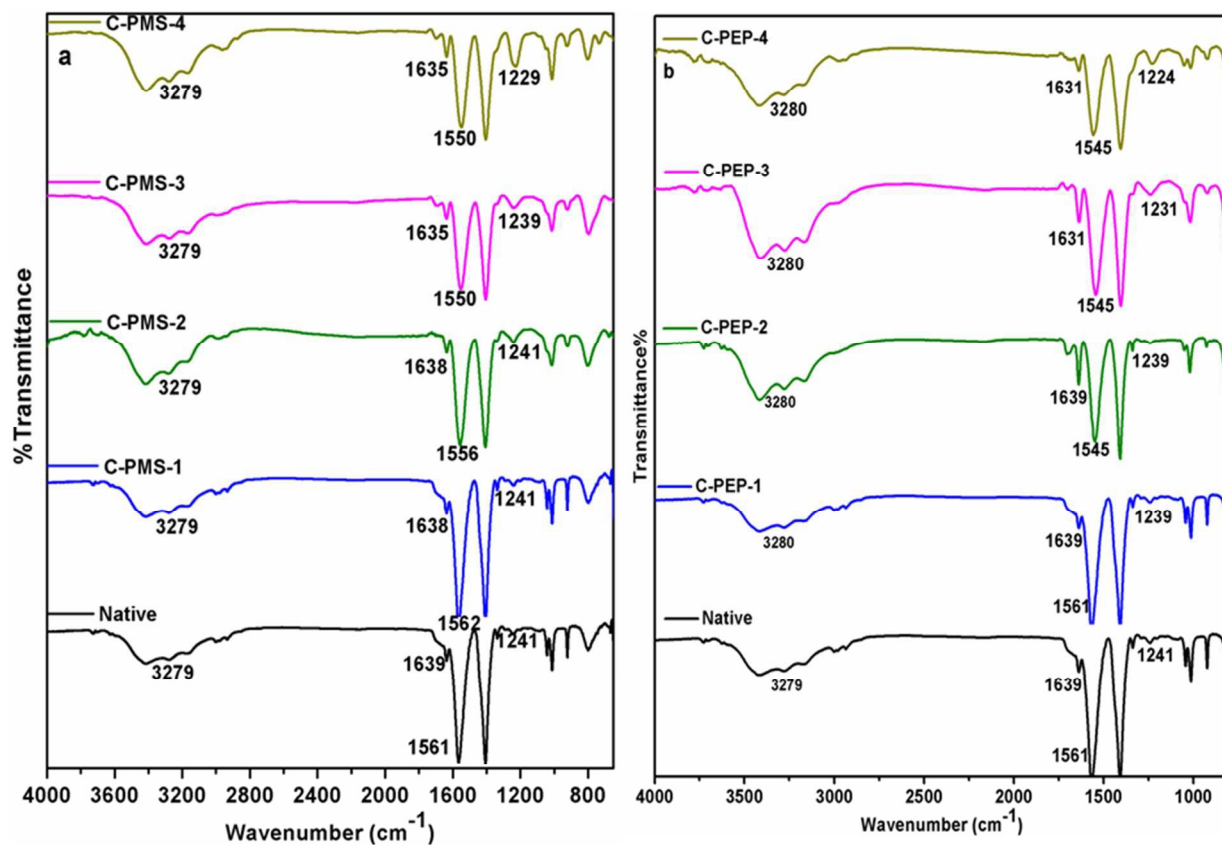


Figure 2. FT-IR spectra representing the changes in the functional groups of collagen treated PILs (a) C-PMS-1 to C-PMS-4 (Collagen: Phosphonium methyl sulfate 1:0.05% to 1:10%) (b) C-PEP-1 to C-PEP-4 (Collagen: Phosphonium diethyl phosphate 1:0.05% to 1:10%)

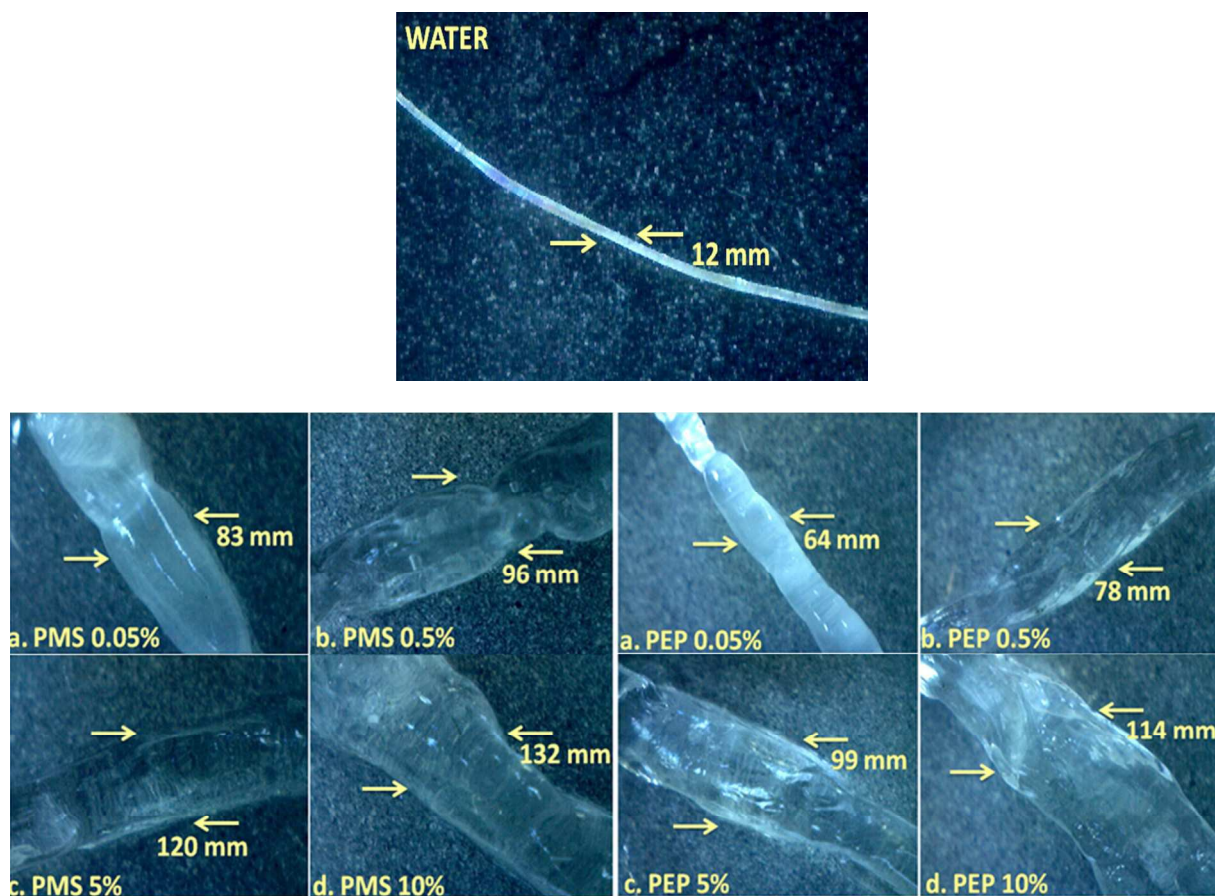


Figure 3. Optical micrographs of (a) Phosphonium methyl sulfate (PMS) 0.05% to 10%  
(b) Phosphonium diethyl phosphate (PEP) 0.05% to 10%

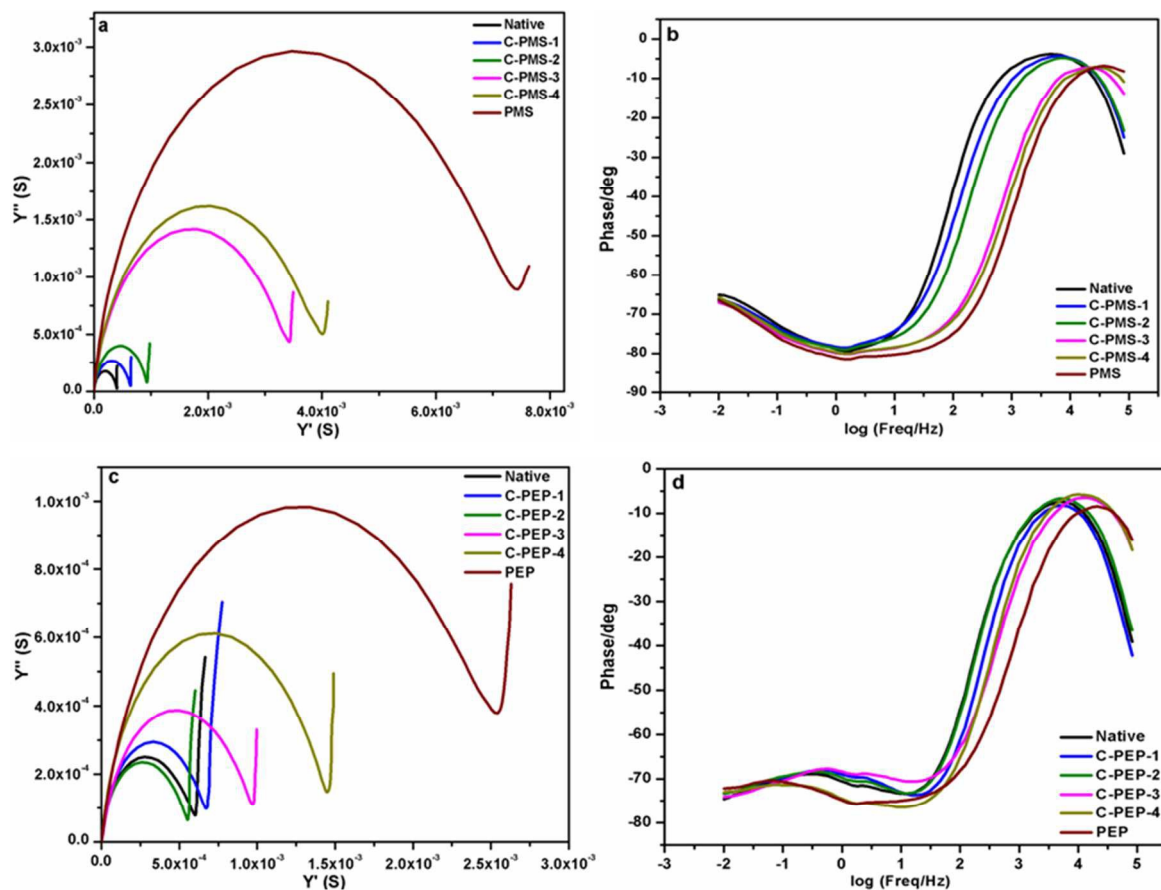
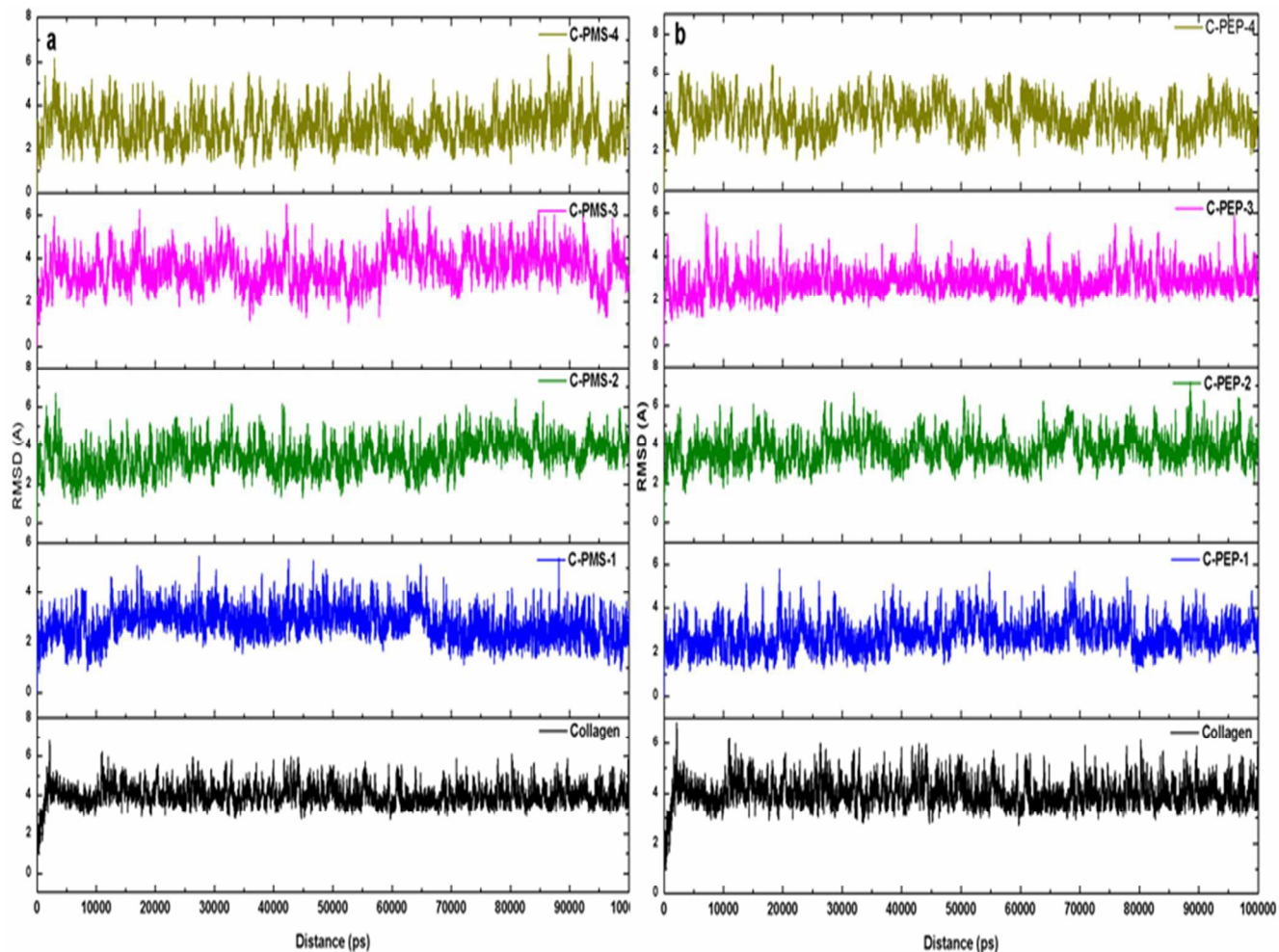
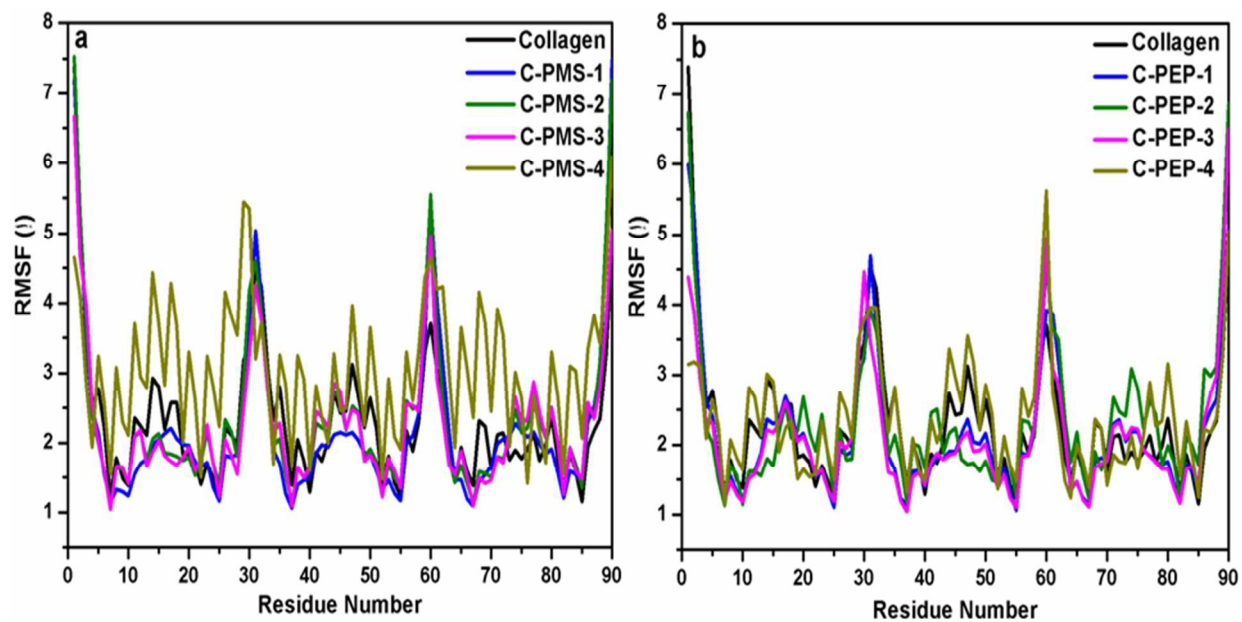


Figure 4. AC impedance analysis of pure collagen with PILs, a. Nyquist plot, b. Bode plot for C-PMS-1 to C-PMS-4 (Collagen: Phosphonium methyl sulfate 1:0.05% to 1:10%), c. Nyquist plot, d. Bode plot for C-PEP-1 to C-PEP-4 (Collagen: Phosphonium diethyl phosphate 1:0.05% to 1:10%)



**Figure 5. RMSD of Collagen and PIL at different concentrations derived by molecular dynamics simulations, (a) C-PMS-1 to C-PMS-4, Collagen: Phosphonium methyl sulfate (1:0.05% to 1:10%), (b) C-PEP-1 to C-PEP-4, Collagen: Phosphonium diethyl phosphate (1:0.05% to 1:10%)**



**Figure 6.** The calculated RMSF values per residue for collagen at different concentrations of PILs, (a) C-PMS-1 to C-PMS-4, Collagen: Phosphonium methyl sulfate (1:0.05% to 1:10%), (b) C-PEP-1 to C-PEP-4, Collagen: Phosphonium diethyl phosphate (1:0.05% to 1:10%)

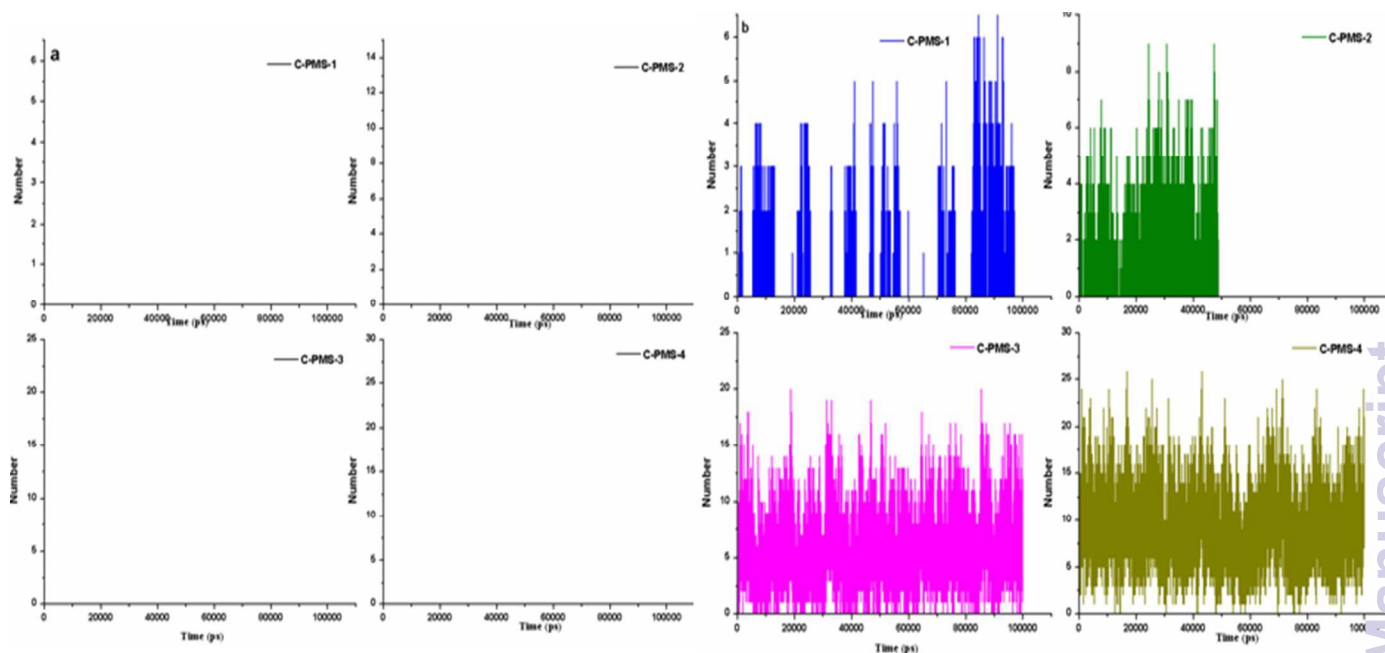


Figure 7. Hydrogen bonding between collagen and PMS, (a) cation and (b) anion of C-PMS-1 to C-PMS-4, Collagen: Phosphonium methyl sulfate (1:0.05% to 1:10%)

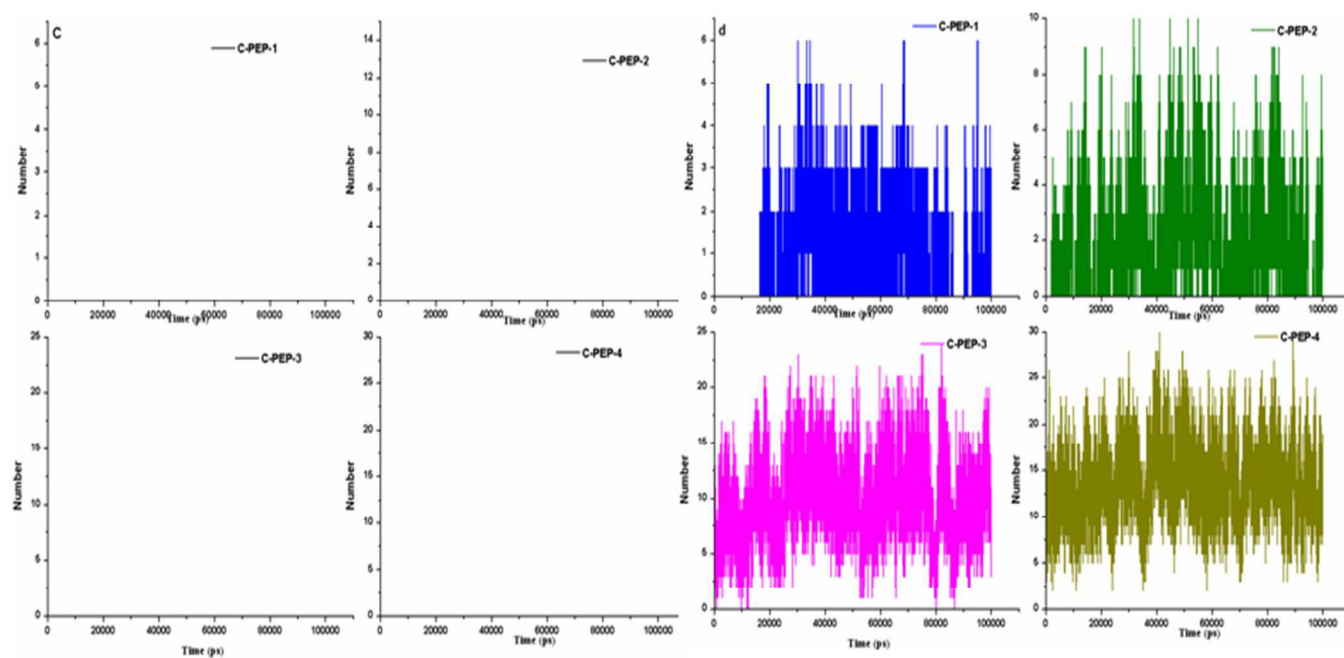


Figure 7. Hydrogen bonding between collagen and PEP (c) cation and (d) anion of C-PEP-1 to C-PEP-4, Collagen: Phosphonium diethyl phosphate (1:0.05% to 1:10%)

RSC Advances Accepted Manuscript

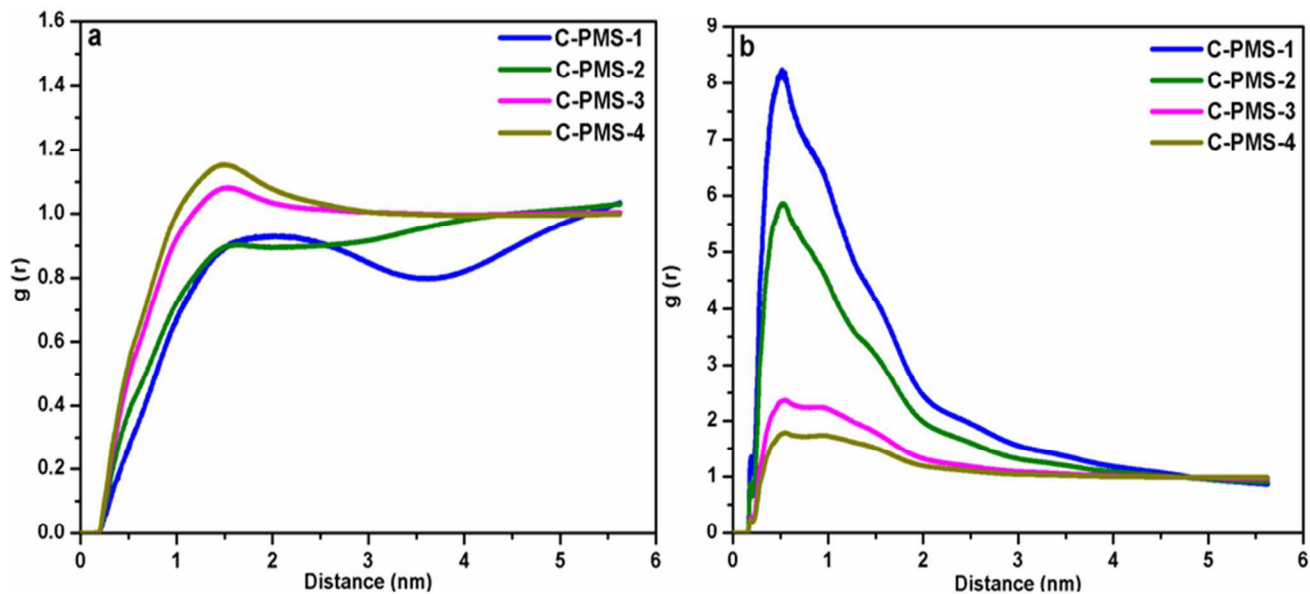


Figure 8. Radial distribution function between collagen and PMS, (a) cation and (b) anion of C-PMS-1 to C-PMS-4, Collagen: Phosphonium methyl sulfate (1:0.05% to 1:10%)

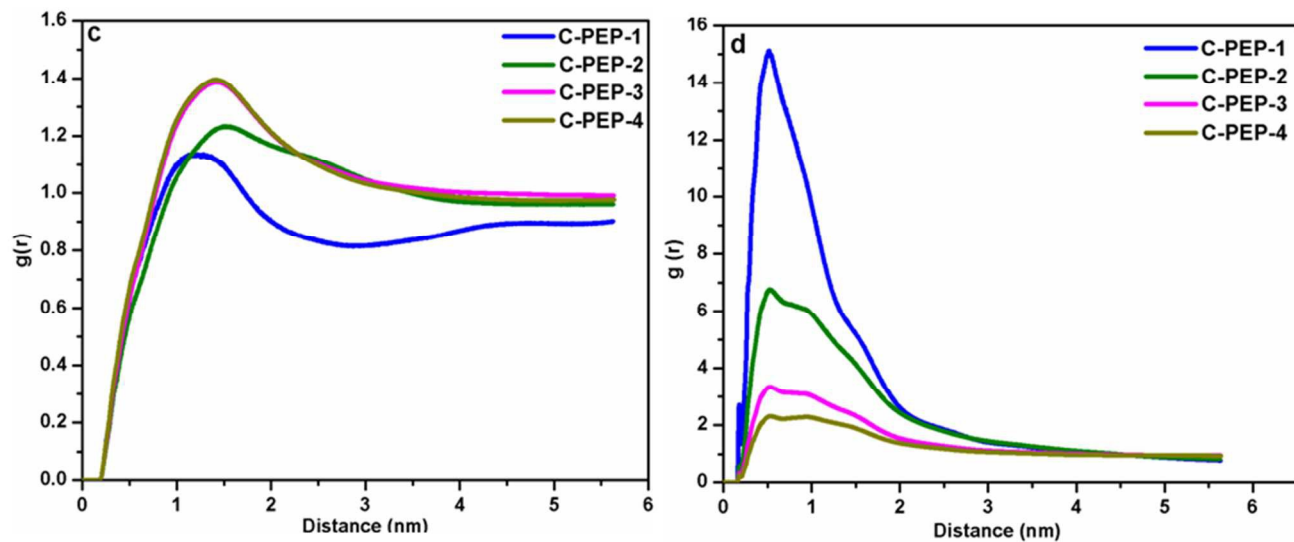


Figure 8. Radial distribution function between collagen and PEP, (c) cation and (d) anion of C-PEP-1 to C-PEP-4, Collagen: Phosphonium diethyl phosphate (1:0.05% to 1:10%)

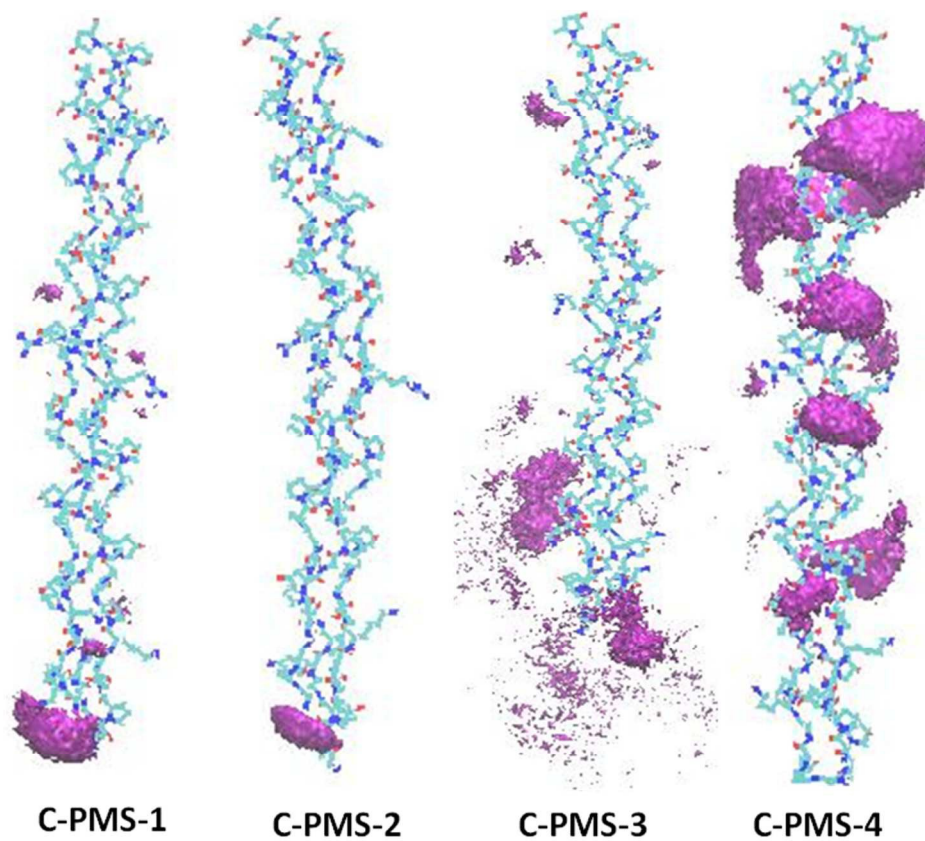
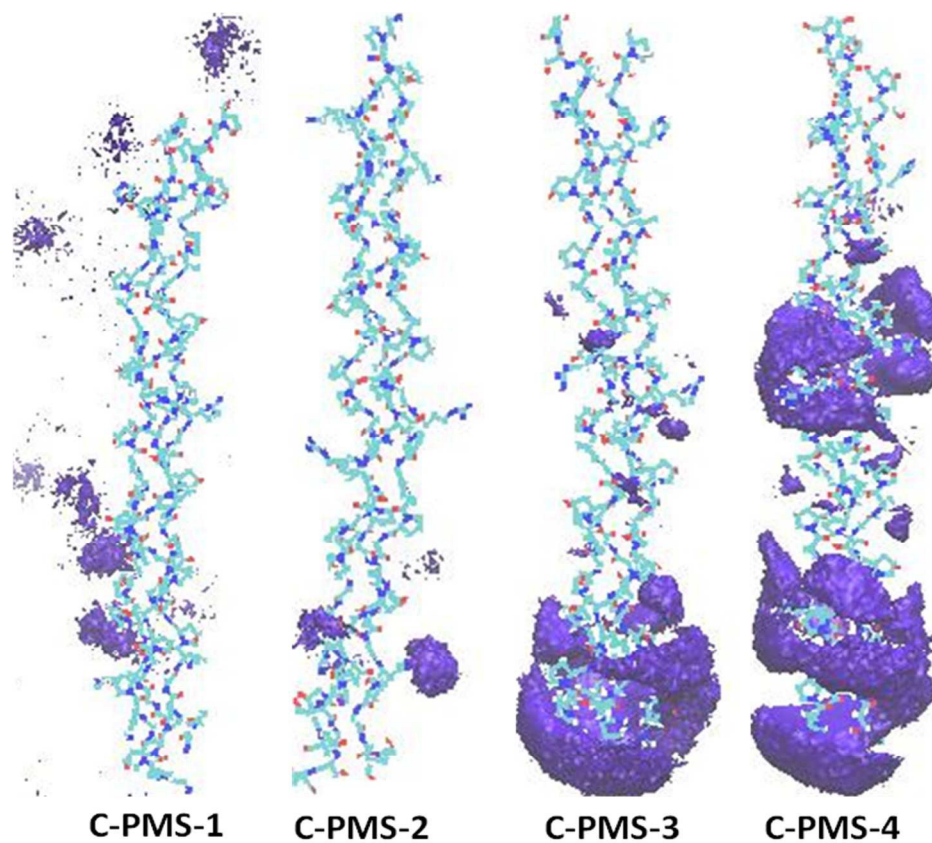
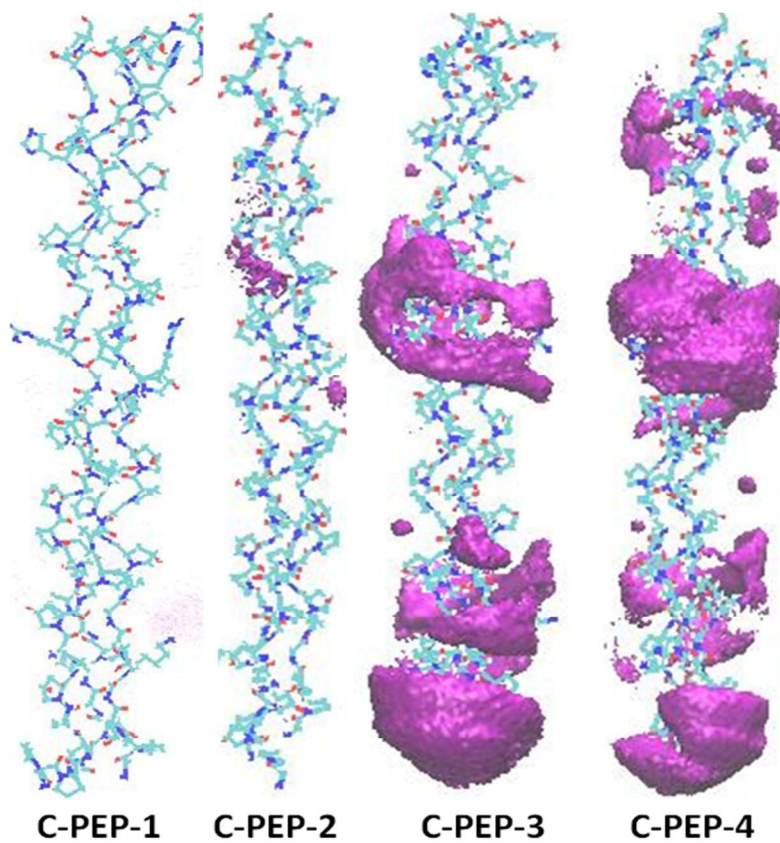


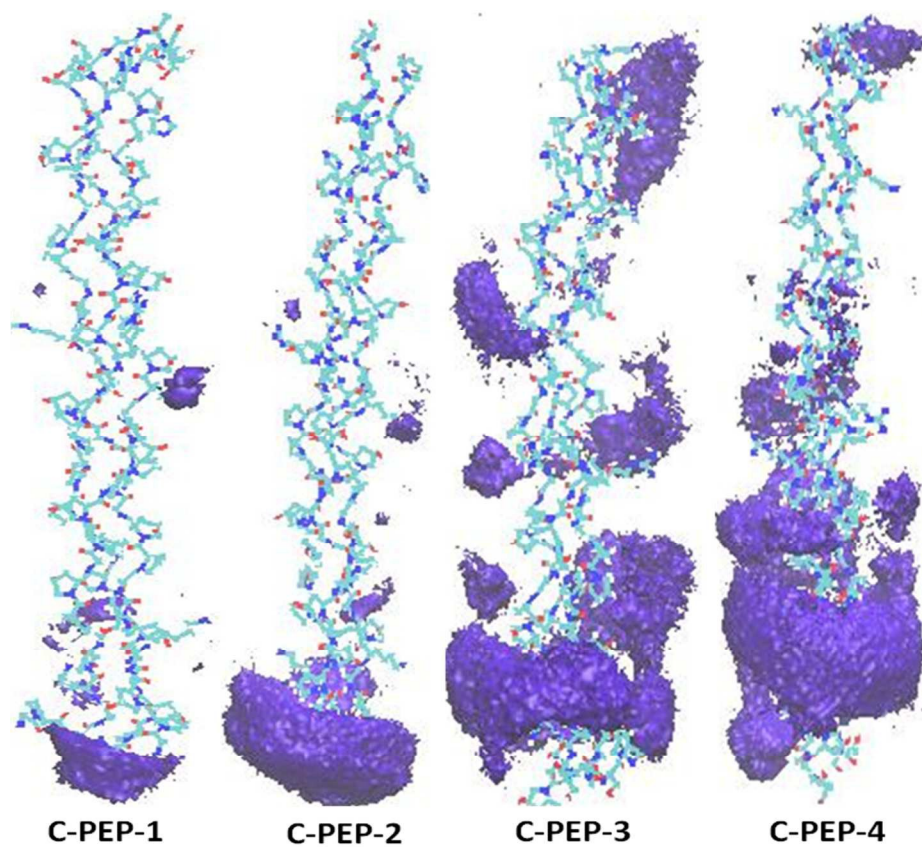
Figure 9a. Spatial distribution function between collagen and cation of C-PMS-1 to C-PMS-4 (1:0.05% to 1:10%)



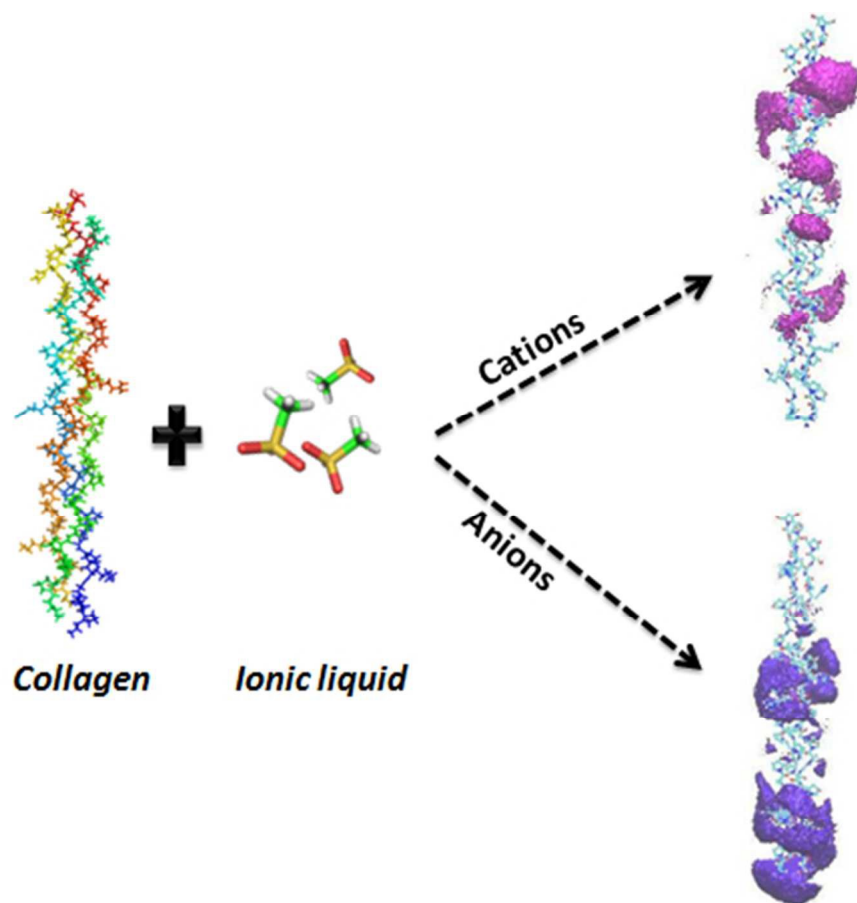
**Figure 9b. Spatial distribution function between collagen and anion of C-PMS-1 to C-PMS-4 (1:0.05% to 1:10%)**



**Figure 9c. Spatial distribution function between collagen and cation of C-PEP-1 to C-PEP-4 (1:0.05% to 1:10%)**



**Figure 9d. Spatial distribution function between collagen and anion of C-PEP-1 to C-PEP-4 (1:0.05% to 1:10%)**



130x119mm (96 x 96 DPI)